Ducted Propellers for High-Speed Underwater Propulsion

S. THURSTON* AND M. S. EVANBAR†
Northrop Corporation, Hawthorne, Calif.

Cavitation limits subcavitating marine propellers to modest forward speeds. At higher speeds the propeller can be designed to operate under cavitating conditions; however, for efficient operation a supercavitating propeller requires a fully developed cavity. The transition zone between subcavitating and supercavitating propellers represents a sizeable region of speed and advance ratio where performance is poor, as neither type of propeller can operate efficiently with partial cavitation. This situation manifests itself as a propulsor performance gap. The analysis presented herein suggests that a high-speed diffusing duct can extend the cavitation-limited speed of the subcavitating propeller to much higher speeds, and that it can thereby operate efficiently within the propulsor performance gap as well as in the region heretofore proprietary to the supercavitating propeller. Both base-ventilated and superventilated ducts are considered in this analysis. As examples, the performance of the two types of high-speed ducted propellers is analyzed for two bodies of revolution at a depth of 10 ft and at velocities of 50 and 70 knots, respectively, and compared with supercavitating propellers. The performance proves to be very attractive.

Nomenclature

A = frontal area, ft²
C_{p_∞} = minimum pressure coefficient = $(p_\infty - p_L)/q_\infty$
C_{p_R} = minimum pressure coefficient based on blade relative conditions = $(p_R - p_L)/q_R$
C_D = total drag coefficient = D/Aq_∞
C_{D_h} = bare-body drag coefficient = D_h/Aq_∞
d_r = rotor diameter, ft
d_h = hub diameter, ft
D_{sh} = shroud drag, lb
D_h = bare-body drag, lb
D = total drag = $D_h(1 + \tau) + D_{sh}$, lb
F = total thrust required for self-propulsion, lb
q_R = blade relative dynamic pressure at inlet station = $(\rho/2g)V_R^2$, lb/ft²
V_∞ = freestream velocity, fps
V_L = blade relative maximum local velocity, fps
V_j = propulsor exit velocity, fps
V_1 = absolute rotor inlet velocity, fps
V_R = blade relative rotor inlet velocity, fps
g = acceleration of gravity, ft/sec²
h = head loss, ft
HP = total shaft power requirement, hp
J = freestream advance ratio = V_∞/Nd_r
K_d = diffusion coefficient = $1 - (V_1/V_\infty)^2$
$\dot{m}$ = weight flow rate, lb/sec
N = rotor speed, rev/sec
N_{lim} = cavitation-limited rotor speed, rev/sec
p_∞ = static pressure in freestream, lb/ft²
p_L = blade minimum local static pressure, lb/ft²
p_R = static pressure on blade at inlet station, lb/ft²
p_v = vapor pressure, lb/ft²
q_∞ = freestream dynamic pressure = $(\rho/2g)V_\infty^2$, lb/ft²
η_j = jet or ideal efficiency = thrust power‡/hydraulic power added to flow = $F(D/D_h)V_\infty/(\dot{m}/2g)(V_j^2 - V_\infty^2)$
η_{hyd} = hydraulic efficiency = hydraulic power added to flow/shaft power = $(\dot{m}/2g)(V_j^2 - V_\infty^2)/550HP$
η_c = shroud drag and thrust-deduction factor = bare-body tow-rope drag/total drag = D_h/D
η_{pc} = propulsive coefficient = thrust power/shaft power = $\eta_j\eta_{hyd}\eta_c = FV_\infty/550\,HP$
τ = thrust-deduction factor = thrust deduction/bare-body tow-rope drag = $[F - (D_h + D_{sh})]/D_h$
ρ = weight density, lb/ft³
σ_R = blade relative cavitation index = $(p_L - p_v)/q_R$
σ_∞ = freestream cavitation index = $(p_\infty - p_v)/q_\infty$

Presented as Paper 67-460 at the AIAA 3rd Propulsion Joint Specialist Conference, Washington, D. C., July 17–21, 1967; submitted August 7, 1967; revision received October 27, 1967.

* Project Chief, Norair Division. Associate Fellow AIAA.
† Senior Engineer, Norair Division.

‡ Shroud drag and thrust deduction not included.

Introduction

IN order to avoid cavitation, efficient subcavitating marine propellers are limited to modest forward speeds. For example, at 10-ft submergence the cavitation-limited speed of a propeller with 90% ideal efficiency is approximately 25 knots at an advance ratio of 1.5, and at a 50-ft submergence is only 40 knots. It is necessary to go to a submergence of approximately 100 ft before the cavitation-free velocity can exceed 50 knots, and even deeper for less efficient propellers. Because the velocities of many present and anticipated surface and underwater vehicles exceed 50 knots, it is apparent that propulsor considerations are extremely important and that the subcavitating propeller is inadequate. The high-speed surface effect ship and hydrofoil are particular examples of craft that operate in the 50- to 100-knot speed range.

Until recent years the forward velocities of most marine craft were within the operating range of subcavitating propellers or represented only a modest extension thereof. As a result there was no urgent requirement for other propulsors. It was generally believed that the next step in propulsor development would be to accept the inevitability of cavitation and design the propeller to operate under cavitating conditions. This belief stimulated considerable research to obtain a fundamental understanding of cavitation and to develop a design approach for supercavitating propellers. However, operation in the transition zone between subcavitating and supercavitating propellers produces poor performance, because neither propeller type can operate efficiently when burdened with partial cavitation. The efficient supercavitating propeller requires a fully developed stable cavity, whereas a subcavitating propeller conceptually remains fully wetted, although in practice some small amount of cavitation can be tolerated.

This propulsor performance gap was first treated by the senior author in 1965,[1] and envelops a wide range of performance, depending on advance ratio and depth of submergence. This region of poor performance is particularly important, as it represents the range of speeds which is now of interest to marine system designers. Therefore, alternative propulsor concepts that can operate efficiently within

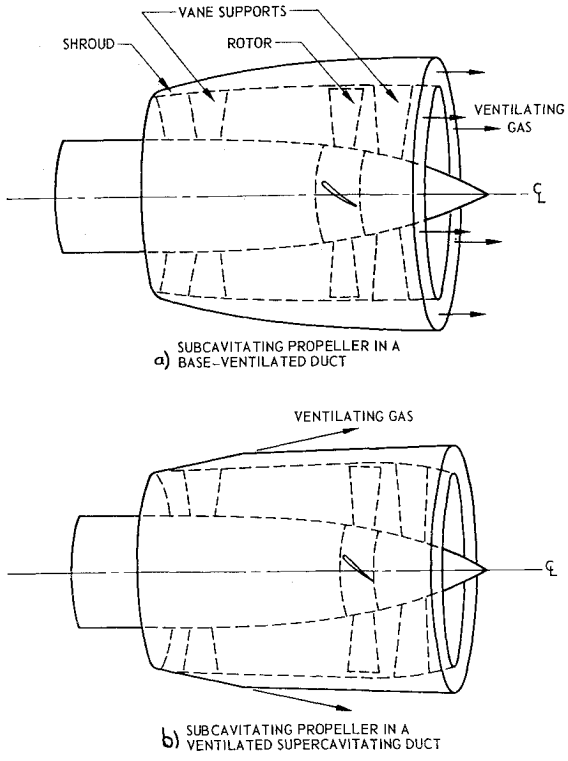

Fig. 1 The two high-speed ducted-propeller configurations.

this performance gap, and techniques that can extend the operating range of efficient subcavitating and supercavitating propellers are of decided importance.

Notwithstanding the recent substantial progress made in supercavitating propeller technology, formidable problems still confront this propeller. These problems result from the following conflicting requirements which must be satisfied: 1) thin blade sections are necessary to achieve good efficiency, and 2) sufficiently rigid sections are needed to transmit efficiently the large amounts of power into the water as useful thrust.

Compromise in the blade design to affect a better structure impairs performance. At present, a satisfactory solution is still not available, especially for large power requirements. As a result there is yet another stimulus to examine other propulsor concepts, not only for operation within the region of the performance gap, but also at higher speeds.

The use of a duct to control the flow behavior can extend the operating range of either the subcavitating or supercavitating propeller. An accelerating-type duct can be used to decrease the local pressure and increase the local velocity entering a supercavitating propeller, and thereby improve its performance at low speeds of advance. However, the complexity and lack of present understanding of three-dimensional cavitating flow within a duct, and the limited potential of the ducted supercavitating propeller have relegated this approach to an inactive status. Alternately, a diffusing duct can be used to increase the local pressure and decrease the local velocity entering a subcavitating propeller, and thereby considerably increase its cavitation-limited forward velocity. Subcavitating ducted propellers have received considerable attention over the past decade, and a substantial analytical and experimental basis is available for design purposes.

This paper explores the performance attainable with a subcavitating propeller operating within a diffusing duct that is designed to operate at high speeds. The diffusing duct controls the flow entering the rotor, to a large extent independently of ambient operating conditions. As the forward speed increases, flow conditions are ultimately reached where the duct itself must cavitate. However, the duct is nonrotative, structurally rigid, and subject to only a portion of the forces acting on the system. The duct, therefore, presents a manageable engineering problem. Two basic types of diffusing ducts are considered, 1) a base-ventilated duct, and 2) a supercavitating, ventilated (super-ventilated) duct. The two ducted propeller types are illustrated in Fig. 1.

An analysis was performed to determine approximate performance regimes and efficiencies of the high-speed ducted propeller. The parametric relationships at design-point were determined by relating mass and momentum considerations internal to the shroud, and by considering the cavitation limitations of the rotor. Some typical vehicles were then selected, and the performance characteristics of specific designs evolved and compared with those of the supercavitating propeller. The numerical results of this analysis and the conclusions derived therefrom are presented in this paper.

The results of the analysis indicate that the high-speed ducted propeller can operate over a significant region of the propulsor performance gap, and also over a large portion of the performance spectrum previously uniquely enjoyed by the supercavitating propeller, but without any identifiable structural limitations. It should be emphasized that the results presented herein are exploratory in nature, and that considerable additional work is required before this concept can be reduced to practice. The present studies analytically establish the feasibility of the high-speed ducted propeller concept and demonstrate its promising performance potential.

Technical Discussion

In order to present a general overview of the potentials of the high-speed ducted propeller, the general considerations involved in its performance are discussed first, and then examples are considered in detail.

Propulsor Performance Gap

The propulsor performance gap, identified in Ref. 1, is illustrated by Fig. 2. Speed of advance is shown as a function of advance ratio for propulsor types with limiting ideal efficiencies of 90% at increasing depths of 10, 50, and 100 ft; the propulsor performance gap is defined by the limit operating lines of a subcavitating propeller on the left and the supercavitating propeller on the right. The limit performance line for the subcavitating propeller is based on the cavitation-limited speed of a 90% efficient propeller with a minimum pressure coefficient on the blade surface (C_{P_R}) of 0.15.[1] The limit operating line for the supercavitating propeller is based on the minimum speed that can support

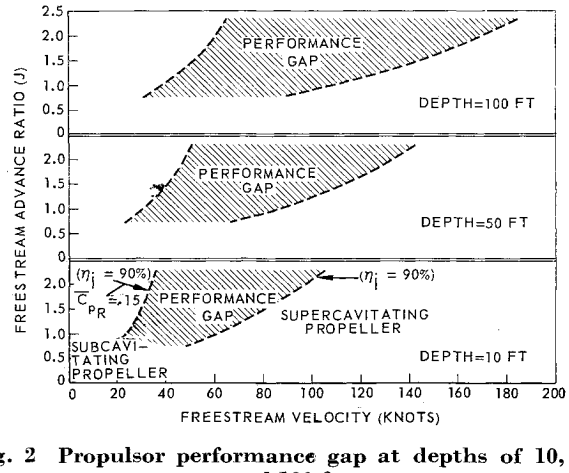

Fig. 2 Propulsor performance gap at depths of 10, 50, and 100 ft.

a stable cavity on a supercavitating propeller.[4] The cavitation-limited speed of the subcavitating propeller increases with depth as expected; however, the minimum operating speed of the supercavitating propeller increases more rapidly with depth due to the disproportionate difficulty of maintaining a fully developed and stable cavity on the supercavitating propeller blades at the higher vapor pressures. The propulsor performance gap, therefore, widens and shifts to higher velocities with increasing depth.

Duct Considerations

The high-speed ducted propeller consists of a subcavitating rotor within a diffusing duct. The duct provides a mechanism to diffuse and control the flow entering the rotor, to a large extent independently of ambient operating conditions, so that the rotor blade need not cavitate. However, as the forward speed increases, the duct itself becomes a problem, and use of conventional subcavitating duct sections would be ineffectual. In order to extend the cavitation-limited speed, the use of base-ventilated duct sections and superventilated duct sections were examined.

The approximate regions of application of conventional subcavitating, base-ventilated, and superventilated diffusing ducts were derived from hydrofoil data, and are shown in Figs. 3 and 4 for a 10-ft submergence. These regions are based on a subcavitating rotor with a diffusion coefficient (K_d) of 0.4. The cavitation-limited speed of the subcavitating duct is approximately 40–50 knots, but with base-ventilated sections can be increased to approximately 80 knots, and thereby can span a significant portion of the performance gap. At speeds above 80 knots, a duct that is designed to accommodate a fully developed cavity on the external surface must be used. Figure 4 illustrates that the superventilated duct can also operate at speeds as low as 35 knots with a stable cavity, and it is possible that forced ventilation may enable operation at lower speeds. Either type of duct can operate within the performance gap region. Consideration of which duct to use, however, involves many other factors, such as shroud drag, ventilation, off-design performance, and requirements for turning and/or acceleration, which would tend to reduce the cavitation-limited speed of the base-ventilated duct. As depth is increased, the subcavitating and base-ventilated ducts can better satisfy the cavitation-limited velocity criteria, and the need for the superventilated duct is delayed to much higher speeds than are presently practical.

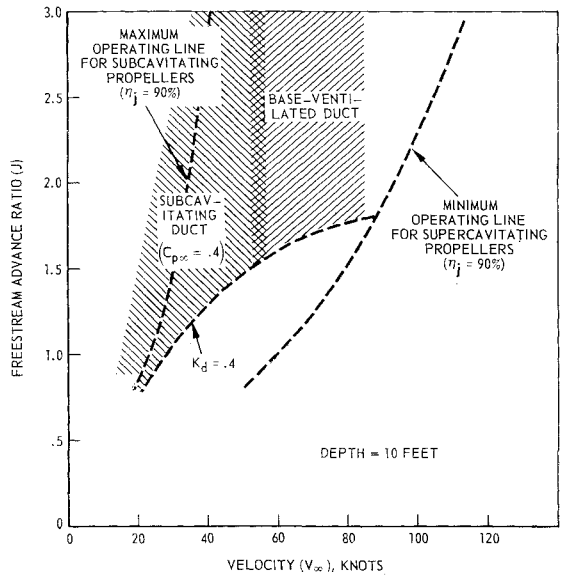

Fig. 3 Regions of operation for diffusing duct propulsors with subcavitating and base-ventilated ducts.

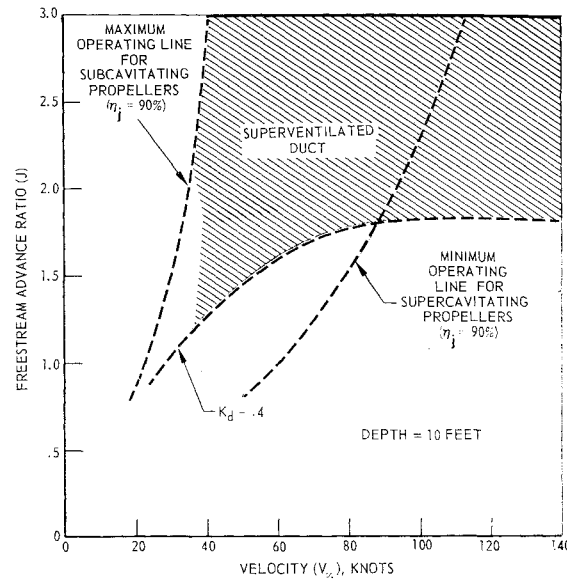

Fig. 4 Regions of operation for diffusing duct propulsors with superventilated ducts.

Another type of ducted-propeller system is the waterjet, which consists of a pump mounted within the vehicle with inlets flush with the body surface or extending outward to form a scoop. The rotor of this propulsor benefits from diffusion; however, waterjet systems, in general, suffer from internal flow losses due to the relatively long ducts required, and from inlet losses which depend on the type of inlet and location. Even relatively small internal losses severely limit the attainable ideal efficiency. This is illustrated in Fig. 5, which shows the ideal efficiency of a waterjet system as a function of jet velocity ratio (V_j/V_∞) for values of velocity head loss factor $2gh/V_\infty^2$. Some typical design values selected for waterjet systems[16,17] are also indicated in Fig. 5. As the waterjet system is located within the vehicle, it occupies usable payload volume, and the water carried detracts further from payload capability. The high-speed ducted-propeller concept presented herein may be considered to be a form of waterjet optimized for maximum efficiency by 1) utilizing a short duct to minimize duct losses, 2) recovering maximum inlet velocity head and mini-

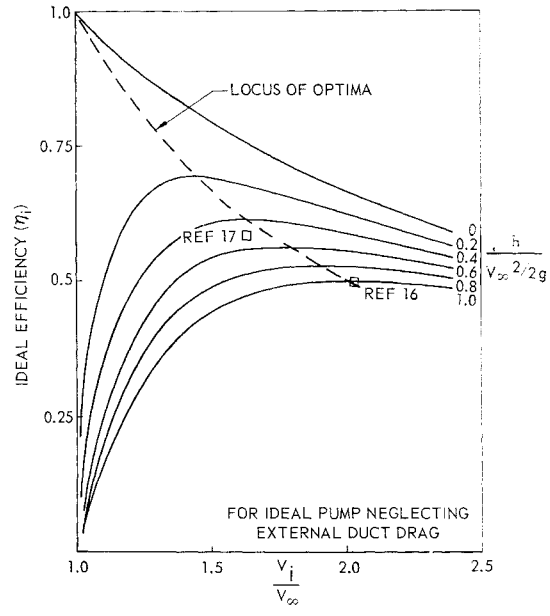

Fig. 5 Waterjet ideal efficiency as a function of velocity ratio for various duct loss factors.

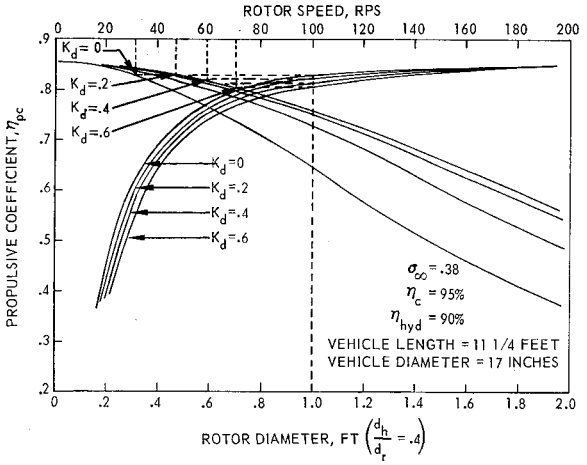

Fig. 6 Variation of propulsive coefficient with cavitation-limited rotor speed and diameter for the base-ventilated duct propulsor configuration at a velocity of 50 knots.

mizing inlet losses, and 3) attaining a high jet or ideal efficiency by inducting large mass flow rates.

Performance Analysis

Preliminary hydrodynamic design studies were performed, based on streamlined underwater bodies of revolution with 8:1 fineness ratios operating at a chord length Reynolds number of 5×10^7 and at a depth of 10 ft. A drag coefficient was determined for such bodies in Ref. 14. The following propulsor configurations were examined:

1) A propeller in a base-ventilated duct operating at 50 knots. Based on the preceding Reynolds number and fineness ratio, the 50-knot vehicle is $11\frac{1}{4}$ ft in length and 17 in. in diameter.

2) A propeller in a superventilated duct operating at 70 knots. This vehicle is 8 ft. in length and 12 in. in diameter.

Performance was determined from simple mass, momentum, and cavitation considerations, the details of which are presented in the Appendix.

Efficiency

The calculated propulsive coefficients for the two foregoing configurations are shown in Figs. 6 and 7 as a function of rotor diameter and rotational speed for various values of diffusion coefficient (K_d). An invariant blade minimum pressure coefficient (0.15) was a blade design criterion for

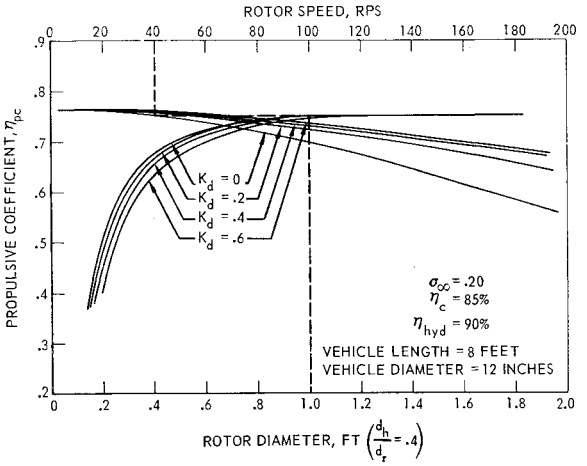

Fig. 7 Variation of propulsive coefficient with cavitation-limited rotor speed and diameter for the superventilated duct propulsor configuration at a velocity of 70 knots.

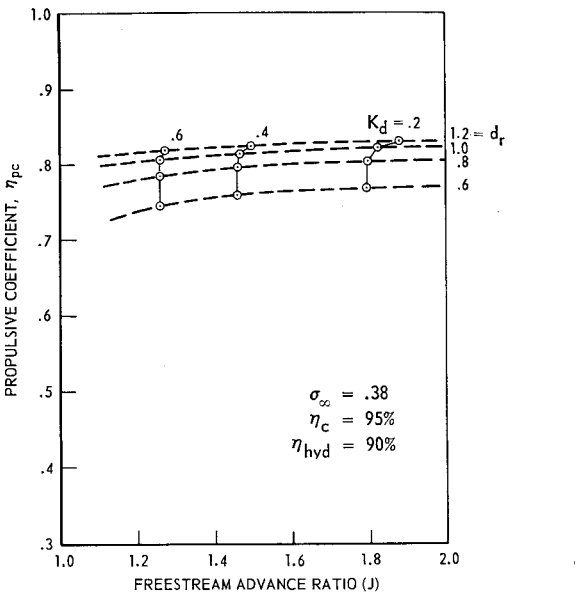

Fig. 8 Variation of propulsive coefficient with advance ratio for the base-ventilated duct propulsor configuration at a velocity of 50 knots.

the range of diffusion coefficients considered, and values of shroud drag and thrust-deduction factor (η_c) and hydraulic efficiency (η_{hyd}) were taken from Refs. 2 and 7. The thrust-deduction factor (τ) is determined implicitly by the choice of drag factor (η_c). A match of design-point rotor speed, rotor diameter, and propulsive coefficient is obtained by entering the figures with a value for one of the three variables and projecting onto the other axes using the corresponding curves of rotor speed and rotor diameter. For example, Fig. 6 demonstrates that a rotor diameter of 1 ft with a duct diffusion coefficient of 0.4 can operate at speeds up to 59 rev/sec with an 81% propulsive coefficient. The maximum propulsive coefficients of 85 and 76% shown in Figs. 6 and 7 are the limiting values and correspond to an ideal efficiency of 100%.

Figures 8 and 9 show the effect of advance ratio on propulsive coefficient for various diffusion coefficients (K_d) and rotor diameters (d_r) for the two propulsor configurations. Considering a diffusion coefficient (K_d) of 0.4, propulsive coefficients as high as 0.82 are indicated for the 50-knot configuration with the base-ventilated duct and 0.75 for the 70-knot configuration with the superventilated duct. For comparative purposes the performance of typical supercavitating propellers obtained from experiment[3] are superimposed on Fig. 9. The 3510 supercavitating propeller attains a propulsive coefficient of 0.69 at 70 knots and an advance ratio of 1.2. At 50 knots, it is necessary for the supercavitating propeller to operate at a relatively inefficient advance ratio and is, therefore, not presented.

Power

Representative values of shroud drag, hydraulic efficiency, and freestream velocities were used to derive Fig. 10, which relates required shaft horsepower to freestream advance ratio. Shroud diffusion coefficient (K_d) and rotor diameter (d_r) are again displayed as parameters. The experimentally determined performance of typical supercavitating propellers is also shown for comparison.

Preliminary estimates indicate that the power requirements for ventilating the shroud cavity are small and, for a first approximation, can be neglected. Either natural or forced ventilation techniques can be used; however, natural ventilation implies operation at or near the surface and, as such, is of interest in applications to planing boats, hydrofoil boats,

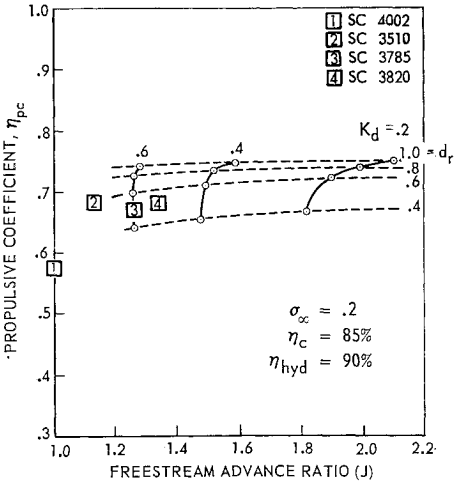

Fig. 9 Variation of propulsive coefficient with advance ratio for the superventilated duct propulsor configuration at a velocity of 70 knots and for supercavitating propellers.

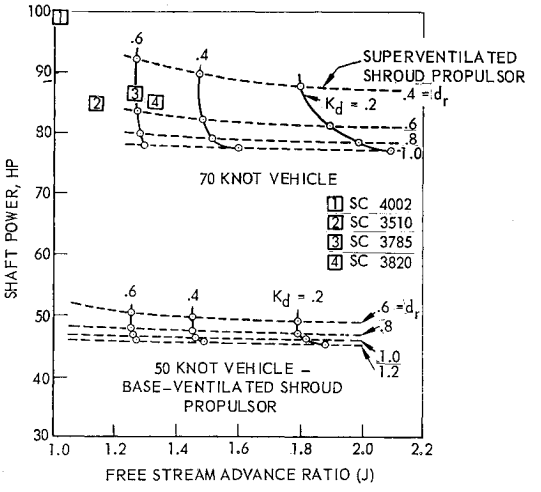

Fig. 10 Variation of shaft power with advance ratio for the base-ventilated duct propulsor configuration and supercavitating propellers at a velocity of 70 knots.

and captured air-bubble, air-cushion craft. Forced ventilation offers an alternative for surface craft and is a requirement for submerged craft. Either gaseous exhaust products from the power plant or compressed air are satisfactory ventilating gases.

Limitations of the Analysis

Since the propeller induces a circulation around the duct, the duct is an integral part of the thrust-producing system. The net drag induced by the propeller on the diffusing duct and on the body is treated in the analysis as a portion of the shroud drag and thrust-deduction factor (η_c). The value of η_c, however, is not known with certainty and was estimated from available experimental data.[2] The effects of control surfaces and other appendages were not considered.

It was assumed that a duct diffusion coefficient of 0.4 is attainable in subcavitating, base-ventilated, and externally cavitating ducts operating at design-point, and that an invariant blade minimum pressure coefficient was the blade design criterion, whereas, in reality, other design factors may take precedence. In addition, much of the shroud analysis in this study was based on two-dimensional hydrofoil technology, as little detailed information dealing with the three-dimensional diffusing annulus is available.

Conclusions

The exploratory analysis presented herein suggests that the high-speed ducted propeller has definite potential for the propulsion of high-speed marine craft. It can operate efficiently within the propulsor performance gap and also in the region now proprietary to the supercavitating propeller. The structural aspects of the subcavitating rotor are satisfactory for transmitting large amounts of power to the water, and the cavitating shroud is not expected to prove a difficult structural problem. Considerable research and development are necessary, however, before this concept reaches the stage of practical application. The potential performance of the high-speed ducted propeller is sufficiently attractive to merit serious and concentrated attention at this time.

Appendix: Procedure and Calculations

The following analysis derives the general interrelationships of the design parameters for a high-speed ducted propeller using simple momentum and energy relations. Supercavitating ventilated and base-ventilated duct propulsor configurations are then evaluated on a fully wetted body with no free surface effects.

The propulsor design variables are 1) rotor speed and blade geometry, 2) speed of advance, and 3) shroud geometry. In addition, the propulsor configuration provides a blading combination of one set of rotor blades followed by a set of stator blades, with a free vortex energy addition by the rotor. The configuration and control stations are shown schematically in Fig. 11. The conditions at station ∞ are assumed those of freestream.

The propulsor design procedure involves calculations which determine 1) steady-state thrust and ventilation power requirements, 2) rotor size and speed relationship dictated by blade cavitation considerations, and 3) shroud drag, shroud diffusion, and propulsive coefficient criteria. Matching the previous parameters at the self-propulsion point is accomplished for a specific design by an iterative process; for the performance analysis, the interrelationships of the basic parameters are derived in closed form to permit a better understanding of their general behavior. Conservative values of shroud drag, induced drag, and hydraulic efficiency are then adopted to evaluate two particular propulsor configurations.

Thrust Requirements

The propulsor exit velocity (V_j) is defined in terms of ideal efficiency (η_j) by

$$\eta_j = 2V_\infty/(V_j + V_\infty) \tag{1}$$

Rewriting,

$$V_j = (V_\infty/\eta_j)(2 - \eta_j) \tag{2}$$

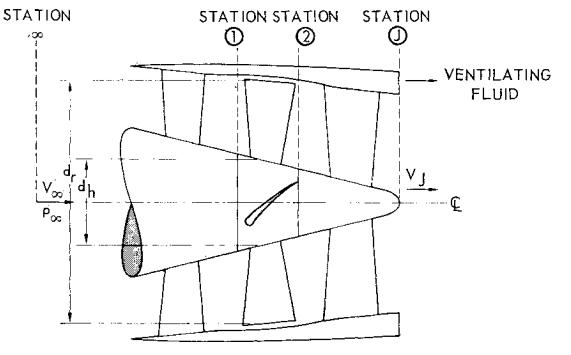

Fig. 11 A schematic showing control stations on the high-speed ducted propeller.

At the self-propulsion point, the thrust is expressed by

$$F = (\dot{m}/g)(V_j - V_\infty) \tag{3}$$

The mass flow rate may be expressed as

$$\dot{m} = (\rho V_1)(\pi/4)d_r^2[1 - (d_h/d_r)^2] \tag{4}$$

A duct diffusion coefficient (K_d) is defined by

$$K_d = 1 - (V_1/V_\infty)^2$$

Subsituting in Eq. (4),

$$\dot{m} = \rho \frac{\pi}{4} V_\infty(1 - K_d)^{1/2} d_r^2 \left[1 - \left(\frac{d_h}{d_r}\right)^2\right] \tag{5}$$

The propulsor thrust is determined from Eqs. (3) and (5) as

$$F = \frac{\rho}{g}\frac{\pi}{4} d_r^2 \left[1 - \left(\frac{d_h}{d_r}\right)^2\right] V_\infty(V_j - V_\infty)(1 - K_d)^{1/2} \tag{6}$$

Rewriting Eq. (2) and substituting in Eq. (6), propulsor thrust is

$$F = q_\infty \pi d_r^2 \left[1 - \left(\frac{d_h}{d_r}\right)^2\right] \frac{(1 - \eta_j)}{\eta_j} (1 - K_d)^{1/2} \tag{7}$$

Rotor-Blade Cavitation Considerations

To satisfy the cavitation requirements of the rotor blade at all conditions of operation, the critical cavitation parameters must be identified and related to rotor speed and geometry, magnitude of shroud diffusion, and speed of advance. By definition, the freestream cavitation index is

$$\sigma_\infty = (p_\infty - p_v)/q_\infty \tag{8}$$

The blade minimum pressure coefficient based on freestream conditions is

$$C_{p\infty} = \frac{p_\infty - p_L}{q_\infty} - \left(\frac{\pi N d_r}{V_\infty}\right)^2 = \left(\frac{V_L}{V_\infty}\right)^2 - 1 - \left(\frac{\pi N d_r}{V_\infty}\right)^2 \tag{9}$$

Relative to the rotating propeller blade, the cavitation index is

$$\sigma_R = (p_L - p_v)/q_R \tag{10}$$

where

$$q_R = \frac{\rho}{2g} V_R^2 = q_\infty \left[(1 - K_d) + \left(\frac{\pi N d_r}{V_\infty}\right)^2\right] \tag{11}$$

The blade minimum pressure coefficient based on relative conditions at the rotor inlet is

$$C_{pR} = (p_R - p_L)/q_R = (V_L/V_R)^2 - 1 \tag{12}$$

By applying Bernoulli's equation between freestream conditions and the station immediately upstream of the propeller,

$$C_{p\infty} = C_{pR}\left[(1 - K_d) + \left(\frac{\pi N d_r}{V_\infty}\right)^2\right] - K_d \tag{13}$$

and from Eqs. (9–12),

$$\sigma_R = \frac{\sigma_\infty + K_d}{(1 - K_d) + (\pi N d_r/V_\infty)^2} - C_{pR} \tag{14}$$

Rewriting

$$\sigma_\infty = (C_{pR} + \sigma_R)\left[(1 - K_d) + \left(\frac{\pi N d_r}{V_\infty}\right)^2\right] - K_d \tag{15}$$

Incipient cavitation is assumed to occur when $\sigma_R = 0$. The cavitation-limited rotor speed is then found by rewriting Eq. (15).

$$N_{\text{lim}} = \frac{V_\infty}{\pi d_r}\left(\frac{\sigma_\infty + K_d(1 + C_{pR}) - C_{pR}}{C_{pR}}\right)^{1/2} \tag{16}$$

The thrust-dependent rotor diameter is given from Eq. (7) by

$$d_r = \left(\frac{F\eta_j}{q_\infty(1 - \eta_j)(1 - K_d)^{1/2}\pi[1 - (d_h/d_r)^2]}\right)^{1/2} \tag{17}$$

A minimum value of 0.4 is selected for the rotor hub-to-tip ratio (d_h/d_r).

Substituting Eq. (17) into Eq. (16), the cavitation-limited rotor speed is expressed in terms of the significant variables:

$$N_{\text{lim}} = 0.518 V_\infty \left(\frac{q_\infty(1 - \eta_j)(1 - K_d)^{1/2}}{C_{pR}F\eta_j} \times [\sigma_\infty + K_d - C_{pR}(1 - K_d)]\right)^{1/2} \tag{18}$$

Maximizing N_{lim} with respect to K_d and solving for K_d,

$$K_d = (2 + 3C_{pR} - \sigma_\infty)/3(1 + C_{pR}) \tag{19}$$

Equation (19) demonstrates that shroud diffusion requirements depend only on freestream cavitation index and on the relative blade minimum pressure coefficient.

Power Considerations

The maximum system efficiency attainable dictates the power requirements at design speed of advance. At design freestream velocity, the power requirement is given by

$$HP = V_\infty\{[D_h(1 + \tau) + D_{\text{sh}}]/\eta_j\eta_{\text{hyd}}\} \tag{20}$$

where the shroud drag term (D_{sh}) includes the shroud drag increment induced by the rotor. A drag factor is defined by

$$\eta_c = D_h/[D_{\text{sh}} + D_h(1 + \tau)] = D_h/D \tag{21}$$

to represent implicitly the drag induced by the rotor as well as the contribution of tow-rope shroud drag to the total drag. Substituting in Eq. (20),

$$HP = V_\infty D_h/\eta_c\eta_{\text{hyd}}\eta_j \tag{22}$$

Ducted-Propeller Configuration Efficiencies

A propulsive coefficient (η_{pc}) can be determined by the product of ideal efficiency, hydraulic efficiency, and a shroud drag factor:

$$\eta_{pc} = \eta_j\eta_{\text{hyd}}\eta_c \tag{23}$$

For conventional blade sections operating at advance ratios within a good design range, a hydraulic efficiency of 90% is reasonable. If approximately 15% of the total vehicle drag is attributed to drag of the supercavitating shroud and thrust deduction at 70 knots, based on Ref. 2, the shroud drag factor (η_c) assumes a value of 85%. η_c approximates 95% for a base-ventilated shroud at 50 knots. These values of η_c are acceptable for ventilated shroud designs, since bodies of revolution with practical shapes and fineness ratios exhibit negligible cavity drag when the base cavitation number is zero.[2,9] The use of hub-ventilated propellers allows a further reduction in cavity drag.

Using the preceding values of hydraulic efficiency and shroud drag factor,

$$(\eta_j)_{50K} = \eta_{pc}/\eta_{\text{hyd}}\eta_c = 1.17\eta_{pc} \tag{24a}$$

$$(\eta_j)_{70K} = 1.31\eta_{pc} \tag{24b}$$

The bare-body drag coefficient based on frontal area is found from experiment[14] to be $C_{D_h} = 0.06$. The total drag coefficient of the body and shroud configuration at the self-

propulsion point is then

$$C_D = C_{D_h}/\eta_c = 0.06/\eta_c \quad (25)$$

Based on a chord length Reynolds number of 5×10^7 and a fineness ratio of 8 to 1, the 50-knot vehicle has a diameter of 17 in., and the 70-knot vehicle, a diameter of 12 in.; substituting in Eq. (25),

$$(C_DA)_{50K} = 0.093/\eta_c = 0.0978 \quad (26a)$$

$$(C_DA)_{70K} = 0.047/\eta_c = 0.0553 \quad (26b)$$

At the self-propulsion point, $F/q_\infty = C_DA$, and Eq. (18) becomes

$$N_{\text{lim}} = 0.518V_\infty \left[\left(\frac{(1-\eta_j)(1-K_d)^{1/2}}{C_DAC_{pR}\eta_j}\right) \times [\sigma_\infty + K_d - C_{pR}(1-K_d)]\right]^{1/2} \quad (27)$$

Substituting Eqs. (24a, 24b, 26a, and 26b) in the preceding relation and simplifying, an expression relating maximum attainable propulsive coefficient to cavitation-limited rotor speed is obtained for the two configurations,

$$(N_{\text{lim}})_{50K} = 129 \left[\left(\frac{1-1.17\eta_{pc}}{\eta_{pc}C_{pR}}\right) \times (1-K_d)^{1/2}[\sigma_\infty + K_d - C_{pR}(1-K_d)]\right]^{1/2} \quad (27a)$$

$$(N_{\text{lim}})_{70K} = 227 \left[\left(\frac{1-1.31\eta_{pc}}{\eta_{pc}C_{pR}}\right) \times (1-K_d)^{1/2}[\sigma_\infty + K_d - C_{pR}(1-K_d)]\right]^{1/2} \quad (27b)$$

The cavitation limitations and total thrust requirements reflected in the previous relations dictate a rotor diameter. Rotor diameter is determined by substituting Eqs. (27a) and (27b) in Eq. (14):

$$(d_r)_{50K} = 0.209[\eta_{pc}/(1-1.17\eta_{pc})(1-K_d)^{1/2}]^{1/2} \quad (28a)$$

$$(d_r)_{70K} = 0.166[\eta_{pc}/(1-1.31\eta_{pc})(1-K_d)^{1/2}]^{1/2} \quad (28b)$$

A match of design-point propulsive coefficient, rotational speed, and diameter can be obtained from the preceding expressions for a given diffusion coefficient (Figs. 6 and 7). A blade minimum pressure coefficient of 0.15 was used.

Ducted-Propeller Configuration Power Requirements

The power required to propel the ducted-propeller configurations is given by Eq. (22),

$$HP = V_\infty\left(\frac{D_h}{\eta_c\eta_{\text{hyd}}\eta_j}\right) = V_\infty\left(\frac{q_\infty C_DA}{\eta_{pc}}\right)$$

Substituting values for the 50- and 70-knot ducted-propeller configurations,

$$(HP)_{50K} = 37.5/\eta_{pc} \quad (29a)$$

$$(HP)_{70K} = 58.2/\eta_{pc} \quad (29b)$$

The preceding expressions are presented graphically in Fig. 10.

References

[1] Thurston, S. and Amsler, R. C., "A Review of Marine Propulsive Devices," Paper 65-482, July 1965 AIAA; also "Review of Marine Propellers and Ducted Propeller Propulsive Devices," *Journal of Aircraft*, Vol. 3, No. 3, May-June 1966, pp. 255–261.

[2] Acosta, A. J., Bate, E. R., and Kiceniuk, T., "Measurements on Fully-Wetted and Ventilated Ring Wing Hydrofoils," Rept. E-138.1, June 1965, Hydrodynamics Lab., California Institute of Technology, Pasadena, Calif.

[3] Hecker, R., "Powering Performance of a Ventilated Propeller," Rept. 1487, June 1961, David Taylor Model Basin Hydromechanics Lab., Washington, D. C.

[4] Tachmindji, A. J. et al., "The Design and Performance of Supercavitating Propellers," Rept. C-807, Feb. 1957, David Taylor Model Basin Hydromechanics Lab., Washington, D. C.

[5] Johnson, V. E., "Theoretical and Experimental Investigation of Supercavitating Hydrofoils Operating Near the Free Water Surface," TR R-93, 1961, NASA Langley Research Center, Hampton, Va.

[6] Lang, T. G. and Daybell, D. A., "Water Tunnel Tests of a Base-Vented Hydrofoil Having a Cambered Parabolic Cross Section," TN P508-10, May 1960, U.S. Naval Ordnance Test Station, China Lake, Calif.

[7] Schulze, W. M. and Erwin, J. R., "NACA 65-Series Compressor Rotor Performance and Comparison with Cascade Results," TN 4130, Oct. 1957, NACA, Washington, D.C.

[8] Clement, E. P. and Blount, P. L., "Resistance Tests of a Systematic Series of Planing Hull Forms," *Society of Naval Architects and Marine Engineers Transactions*, Vol. 71, 1963, pp. 491–579.

[9] Ho, H. T. and Chen, C. F., "Low Drag Supercavitating Axisymmetric Bodies," TR 121-2, June 1963, Hydronautics Inc., Laurel, Md.

[10] Kermeen, R. W., "Experimental Investigations of Three-Dimensional Effects on Cavitating Hydrofoils," Rept. 47-14, Sept. 1960, Engineering Div., California Institute of Technology, Pasadena, Calif.

[11] Starley, S. E. and Johnson, V. E., "Low Drag Base-Vented Hydrofoils Designed for Operation Near the Free Surface," TR 001-15, Nov. 1963, Hydronautics Inc., Laurel, Md.

[12] Smith, A. M. O. and Pierce, J., "Exact Solution of the Neumann Problem—Calculation of Noncirculatory Plane and Axially-Symmetric Flows About or Within Arbitrary Boundaries," Rept. ES 20988, April 1958, Douglas Aircraft Co., Santa Monica, Calif.

[13] Schlichting, H., *Boundary Layer Theory*, 4th ed., McGraw-Hill, New York, 1960.

[14] Hoerner, S. F., *Fluid-Dynamic Drag*, Midland Park, N.J., 1958.

[15] Yao-Tsu Wu, T., "Propeller Theory and Marine Propulsion," *AIAA Symposium on Modern Developments in Marine Sciences*, April 1966.

[16] Traksel, J. and Beck, W. E., "Waterjet Propulsion for Marine Vehicles," *Journal of Aircraft*, Vol. 3, No. 2, March-April 1966, pp. 167–173.

[17] Johnson, V., "Water Jet Propulsion for High-Speed Hydrofoil Craft," Paper 64-306, June 1964, AIAA; also *Journal of Aircraft*, Vol. 3, No. 2, March-April, pp. 174–179.

[18] "Ship Propulsion and Hydroelasticity," *Fourth Symposium on Naval Hydrodynamics*, ACR-73, Vol. 1, Office of Naval Research, Aug. 1962.